

AD-A085 858 AIR FORCE WRIGHT AERONAUTICAL LABS WRIGHT-PATTERSON AFB OH F/O 11/4  
FAILURE ANALYSIS OF COMPOSITE LAMINATES WITH A FASTENER HOLE.(U)  
MAR 80 S R SONI  
UNCLASSIFIED AFVAL-TR-80-0010

AIR FORCE WRIGHT AERONAUTICAL LABS WRIGHT-PATTERSON AFB OH P/O 11/4  
FAILURE ANALYSIS OF COMPOSITE LAMINATES WITH A FASTENER HOLE.(U)  
MAR 80 S R SONI  
AFWAL-TR-80-4010

**ML**

104

AC  
ACF:000000

END  
DATE  
FILMED  
8-80  
DTIC

AFWAL-TR-80-4010

16-11-77

(2)

ADA 085858

# FAILURE ANALYSIS OF COMPOSITE LAMINATES WITH A FASTENER HOLE

Som R. Soni

Mechanics and Surface Interactions Branch  
Nonmetallic Materials Division

March 1980

JUN 2 1980  
A

TECHNICAL REPORT AFWAL-TR-80-4010

Final Report for Period September 1978 to August 1979

Approved for public release; distribution unlimited.

DDC FILE COPY

MATERIALS LABORATORY  
AIR FORCE WRIGHT AERONAUTICAL LABORATORIES  
AIR FORCE SYSTEMS COMMAND  
WRIGHT-PATTERSON AIR FORCE BASE, OHIO 45433

80 6 23 112

NOTICE

When Government drawings, specifications, or other data are used for any purpose other than in connection with a definitely related Government procurement operation, the United States Government thereby incurs no responsibility nor any obligation whatsoever; and the fact that the government may have formulated, furnished, or in any way supplied the said drawings, specifications, or other data, is not to be regarded by implication or otherwise as in any manner licensing the holder or any other person or corporation, or conveying any rights or permission to manufacture, use, or sell any patented invention that may in any way be related thereto.

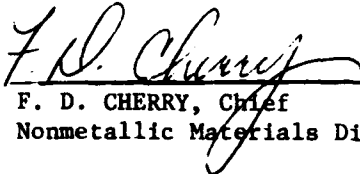
This report has been reviewed by the Information Office (OI) and is releasable to the National Technical Information Service (NTIS). At NTIS, it will be available to the general public, including foreign nations.

This technical report has been reviewed and is approved for publication.



S. W. TSAI, Project Engineer & Chief  
Mechanics & Surface Interactions Br.  
Nonmetallic Materials Division

FOR THE COMMANDER



F. D. CHERRY, Chief  
Nonmetallic Materials Division

"If your address has changed, if you wish to be removed from our mailing list, or if the addressee is no longer employed by your organization please notify AFVAL/MLRM, W-PAFB, OH 45433 to help us maintain a current mailing list".

Copies of this report should not be returned unless return is required by security considerations, contractual obligations, or notice on a specific document.

SECURITY CLASSIFICATION OF THIS PAGE (When Data Entered)

DD FORM 1473 EDITION OF 1 NOV 68 IS OBSOLETE

SECURITY CLASSIFICATION OF THIS PAGE (When Data Entered)

392662

UNCLASSIFIED

SECURITY CLASSIFICATION OF THIS PAGE(When Data Entered)

ply orientations. The ultimate laminate failure strength is based on the last ply failure stress. The resulting predictions of strength are found to be conservative as compared to experimental values.

UNCLASSIFIED

SECURITY CLASSIFICATION OF THIS PAGE(When Data Entered)

FOREWORD

This report describes the inhouse effort conducted in the Mechanics and Surface Interactions Branch (MLBM), Nonmetallic Materials Division (MLB), Air Force Materials Laboratory, Wright-Patterson Air Force Base, Ohio, under the National Research Council-Air Force Systems Command research associateship program.

The work reported herein was performed during the period 15 September 1978 to 1 August 1979. Dr. Stephen W. Tsai (AFWAL/MLBM) was the Project Engineer and Dr. S. R. Soni was the NRC-AFSC Senior Postdoctorate Research Associate.

The author wishes to express his deep sense of gratitude to Dr. S. W. Tsai for his extremely fruitful guidance in the course of his work. The author is grateful to Mr. Nick Negaard, Structures Information Center, Flight Dynamics Laboratory, for help in the use of NASTRAN.

APPROVED FOR
THIS WORK
DDC YES
UNCLASSIFIED
JUSTIFIED
BY
DATE
DIST.
A

AFWAL-TR-80-4010

## TABLE OF CONTENTS

SECTION	PAGE
I INTRODUCTION	1
II PROBLEM DEFINITION	4
1. Finite Element Model	4
2. Failure Criterion	5
3. Laminate Material Properties	6
4. Numerical Results and Discussion	6
5. Example	9
III CONCLUSIONS	11
REFERENCES	12
APPENDIX	15

## LIST OF ILLUSTRATIONS

FIGURE		PAGE
1	Laminate with Coordinate Axis and Dimensions	22
2	Finite Element Grid of the Laminate	23
3	Comparison Between Finite Element and Closed Form (with a Finite Width Correction Factor) Results for $\sigma_x$ in Free Hole Boundary Condition	24
4	Strength Ratio $P/N_0$ versus Diameter to Width Ratio D/W of the $(0,90,+\underline{0}45)_s$ Laminate	25
5	Strength Ratio $P/N_0$ versus Diameter to Width Ratio D/W of the $(0,90,(\underline{+}45)_2)_s$ Laminate	26
6	Strength Ratio $P/N_0$ versus Diameter to Width Ratio D/W of the $(0_2,\underline{+}45)_s$ - Laminate	27
7	Strength Ratio $P/N_0$ versus Diameter to Width Ratio D/W of the $(0,90)_{2s}$ Laminate	28
8	Strength Ratio $P/N_0$ versus Diameter to Width Ratio D/W of the $(90_2,\underline{+}45)_{2s}$ Laminate	29
9	Strength Ratio $P/N_0$ versus Diameter to Width Ratio D/W of the $(\underline{+}45)_{2s}$ Laminate	30
10	Strength Ratio $P/N_0$ versus Diameter to Width Ratio D/W of the $(0^\circ)$ Laminate	31
11	Strength Ratio $P/N_0$ versus Diameter to Width Ratio D/W of the $(90^\circ)$ Laminate	32



## LIST OF ILLUSTRATIONS (CONTINUED)

FIGURE		PAGE
12	Strength P versus Diameter to Width Ratio D/W of Various Angle Ply Laminates	33
13	Strength N versus Hole Load to Total Load Ratio of AS-3501 Material (0,90, <u>+</u> 45) <sub>s</sub> Laminate, D/W = .125	34
14	Projection of Failure Mode Based on Stress Components at the Weakest Point and Ultimate Failure Strengths of the Composite Laminate	35
	(a) (90 <sub>2</sub> , <u>+</u> 45) <sub>s</sub> Laminate, D/W = .125. Net Tension Failure.	35
	(b) (0°) Laminate, D/W = .125, Tearing off.	36
	(c) (0,90) <sub>2s</sub> Laminate, D/W = .125, Shear Out.	37
	(d) (90°) Laminate, D/W = .125, Net Tension.	38
	(e) (0,90, <u>+</u> 45) <sub>s</sub> Laminate, D/W = .125, Compressive.	39

LIST OF TABLES

TABLE		PAGE
1	Material Properties of Different Laminates in SI-Units	18
2	Failure Strengths of Different Laminates	19
3	Comparison Between Experimental and Predicted Strengths of $(0,90,45)_S$ - AS-3501 Laminate D/W = .125	20
4	Comparison Between Experimental and Predicted Strength Ratios for T300/5208 Laminate, D/W = .125	21

NOTATIONS

C	Moisture contents (by weight)
Comp.	Compressive
D	Diameter of the hole
E	Distance of the center of the hole from the nearer edge
$F_{ij}$	Tensor polynomial failure criterion coefficients dependent upon the ply strengths in different directions
$f_1$	$(P/N_0)_{Exp}/(P/N_0)_{predicted}$ (Dry)
$f_2$	$(P/N_0)_{Exp}/(P/N_0)_{predicted}$ (Moist)
h	Thickness of the laminate
L	Length of the laminate
N	Uniaxial applied stress (Figure 1)
N'	Uniaxial applied stress (Figure 1)
$N_0$	Strength of unnotched laminate in tension
$N_0^C$	Compressive strength of unnotched laminate
$N_0^S$	Shear strength of unnotched laminate
NT	Net tension
P	Uniaxial applied stress (Figure 1) Predicted strength of the notched laminate
$Q_{ij}$	Modulus matrix
$S_i^j$	Strength of $i^{th}$ ply at the $j^{th}$ element

AFWAL-TR-80-4010

$S_{cf}$	Stress concentration factor
$\Delta T$	Temperature difference
$W$	Width of the laminate
$x^i$	Strength of the strongest ply at the $i^{th}$ element
$(x,y)$	Cartesian coordinate axis
$(\epsilon_x, \epsilon_y, \epsilon_{xy})$	Strain components
$(\sigma_x, \sigma_y, \tau_{xy})$	Stress components
$\sigma$	Uniaxial applied stress

## SECTION I

### INTRODUCTION

With the advent of composite materials and their enormous use in highly stressed lightweight constructions, it has become necessary to have a deep insight into the failure of composite bolted joints. There have been very few investigations towards the failure analysis of bolted joints. Some of the papers in this area have been reported in Reference 1, which uses a finite element technique and the average radial stress over a characteristic distance  $d$  (from the hole boundary) as a stress level to predict the failure strength of the laminate. This parameter  $d$  is considered as a material property. Recently Garbo and Ogonowski (Reference 2) used the characteristic distance concept of Whitney and Nuismer (Reference 3) and Wu (Reference 4) to determine the strength of mechanically fastened composite joints. According to this hypothesis they chose a characteristic distance  $d$  away from the hole and used the stress level at this distance to compute the failure loads of different laminates by the Tsai - Hill criterion (References 5,6). The laminate failure was assumed to occur when the first ply fiber fails. The analytical results compared with experimental data in this report tended to favor this technique.

The idea behind taking the average stress over a fixed range or an effective stress to compute the failure strength of the notched laminate emerged from the fact that the maximum theoretical value of the localized stress around the hole is higher than the experimental value. The calculated stress concentration factors apply mainly to ideal elastic materials and depend upon the geometry or form of the abrupt change in section. However, in applications involving real materials, the significance of a stress concentration factor is not indicated satisfactorily by the calculated value. It is found through experience that the effective stress value that indicates impending structural damage of a member depends upon

the characteristics of the material and on the nature of the load and the geometry of the stress raiser. Consequently, the effective value of stress concentration is obtained by multiplying the nominal stress by an effective stress concentration factor, which is less than the calculated stress concentration factor (Reference 7). The determination of effective stress concentration factor requires experimental data.

The present work is concerned with the investigation of strength of composite laminates having a through the thickness loaded circular hole. The hole is assumed to be filled with a rigid core to simulate the bolted joint situation. The finite element technique coupled with the classical laminated plate theory has been used in computing the stress distribution in the laminate. The displacement boundary conditions are applied to the rigid core to represent load at the bolted joint. Tensor polynomial failure criterion (Reference 8) has been applied to predict the ultimate failure strength of notched laminates. According to this criterion the combination of stresses that causes the lamina failure can be represented by a surface in stress space i.e.,

$$F_{11}\sigma_1^2 + F_{22}\sigma_2^2 + F_{66}\sigma_6^2 + 2F_{12}\sigma_1\sigma_2 + F_{11}\sigma_1 + F_{22}\sigma_2 = 1 \quad (1)$$

where  $F_i$ s are evaluated from axial, transverse and shear strengths of the lamina and  $\sigma_1$ ,  $\sigma_2$  and  $\sigma_6$  are inplane axial, transverse and shear stress components, respectively, at a point (Reference 9).

Prior to the application of this criterion to a composite laminate, it is necessary to define how to treat the lamina failure that occurs before the total laminate failure. There are various ways of treating the laminate stiffness after lamina failure (Reference 10). In the present study it has been assumed that laminate fails when last ply failure occurs at the weakest point.

The tensor polynomial failure criterion (Reference 8) was used to obtain the failure strength of each ply in the laminate. The failure

AFWAL-TR-80-4010

strength of strongest ply at the weakest point of the laminate was considered as the ultimate failure strength of the laminate. Experimental results are available for a limited number of laminates and show a wide scatter in strength.

Apart from the failure strengths of the loaded hole laminate, the present study predicts the possible mode of failure. The different modes of failure observed in this analysis are given in Figure A1.

## SECTION II

### PROBLEM DEFINITION

Figure 1 shows a laminate with a fastener hole and possible simple uniaxial loads. The following three combinations of loading conditions can be investigated:

- i. Loaded hole ( $N' = 0$ )
- ii. Partial load acting at the hole ( $N' \neq 0$ ,  $P \neq 0$ )
- iii. Free Hole ( $P = 0$ )

The loaded hole condition resembles the bolted joint situation and is of great practical importance in engineering applications. The emphasis of the present investigation is on this condition, though the other two conditions are dealt with for the purpose of comparison between the predicted strength and already available experimental strength of laminates. There exist no reliable close form solutions for the stress analysis of the laminate with loaded hole conditions. Finite element technique has been utilized to conduct the stress analysis of the laminate. To simulate loaded hole condition, various boundary constraints were tried in the finite element analysis. It was found that the boundary conditions with zero radial displacement along the semicircular boundary in contact with the bolt and known applied tensile load at the opposite plane edge represent loaded hole conditions.

#### 1. FINITE ELEMENT MODEL

A notched laminate as shown in Figure 1 is under investigation for stress analysis by the finite element technique, using the NASTRAN computer code. The stress distribution in the laminate is computed by considering half of the laminate, thereby taking the advantage of geometric symmetry about x-axis. The half of the laminate is divided into 372 quadrilateral and triangular elements. The loaded hole conditions were simulated by taking radial displacement along the bolt contact



semicircular boundary as zero and applying known tensile load at the opposite plane edge. This transpires that the model assumes a rigid frictionless bolt and the contact surface between the bolt and laminate is semicircular. Further it was assumed that no lateral pressure was acting at the laminate. The gross laminate material properties using the laminated plate theory were used. A finite element grid plot as obtained during the NASTRAN computations is given in Figure 2. Various numerical exercises with different finite element grids showed that the present model is good enough to give acceptable results for all practical purposes.

## 2. FAILURE CRITERION

The stress components, obtained by the finite element analysis, at each point around the hole are used to predict the maximum allowable tensile stress in individual lamina through the use of tensor polynomial failure criterion (Reference 9). This yields as many failure strengths as the ply angle orientations in the laminate under consideration. The ultimate failure of the laminate is assumed to take place at the weakest point when the strongest lamina fails. This is illustrated by the following example:

Assume that the laminate under consideration has 4 angle ply orientations and there are 20 elements at each of which the average state of stress is known to be  $(\sigma_1^i, \sigma_2^i, \sigma_6^i)$   $i = 1, 2, 3, \dots, 20$ . The use of stress components corresponding to each element in the failure criterion yields four strengths  $[S_1^i, S_2^i, S_3^i, S_4^i]$ ,  $i = 1, 2, \dots, 20$  one pertaining to each angle ply. The strongest lamina strength  $x^i$  for each element is given by

$$x^i = \text{maximum } [S_1^i, S_2^i, S_3^i, S_4^i]$$

$$i = 1, 2, \dots, 20$$

The ultimate failure strength  $P$  of the laminate is assumed to be given by

$$P = \text{min. } (x^1, x^2, \dots, x^{20})$$

and the weakest point is in the element to which this value corresponds. In case there is more than one element having the ultimate strength  $P$ , the element with minimum of second largest angle ply strength will be considered as the area of failure.

### 3. LAMINATE MATERIAL PROPERTIES

The analysis of composite laminates is limited to those stacking sequences which have midplane symmetry, i.e., the ply orientations in the lower half of the laminate are the reflections of those of the upper half plies. Such laminates are assumed to behave like homogeneous anisotropic plates. The procedure of computing the stiffness properties of multidirectional laminates is described in Reference 11. The effective modulus of the composite laminate is simply the arithmetic average of the moduli of constituent plies. For T300/5208 material, the values of nonzero elements of modulus matrix are given in Table 1 for relevant laminate ply orientations. The ply strengths of different laminates for tensile, compressive, and shear loadings are given in Table 2. These values are calculated using the tensor polynomial failure criterion.

### 4. NUMERICAL RESULTS AND DISCUSSION

A computer program was written to generate the grid points and element topologies for the use in finite element calculations of the problem. The physical dimensions were taken to be the same as those in Reference 12 with a variation in the diameter  $D$  of the hole and are stated in Figure 1. In order to check the finite element model the stress components at all the elements for isotropic laminate with a free hole boundary condition were obtained. Values of  $\sigma_x$  along the line normal to x-axis and passing through the center of the hole are plotted in Figure 3. For comparison, the axial stress component  $\sigma_x$  computed by using the infinite isotropic plate formulation (Reference 13), with finite width correction factor is also given. The agreement of results is very good.

It is found that the stress components near the point of stress concentration vary rapidly. Consequently, the computed average stresses over the element containing that point are a bit lower than the actual stress level. Efforts are made to discretize the laminate in such a fashion that the areas of the elements in the critical region are so small that the results are very close to the exact values. Since average stress components over the elements are used in the failure criterion, the inaccuracy would be transmitted into the failure loads. However, for all practical purposes, the results are within acceptable limits.

The Appendix explains the procedure of obtaining the notch insensitive strengths of the notched laminates. These are used in all the diagrams, wherever applicable, to provide the upper limits of the notched laminate strengths. While conducting the finite element analysis for this problem we obtain the stress distribution at various points of the loaded hole laminate. We are more interested in the stress levels at points around the circumference of the hole which is the region of stress concentration and impending failure. The use of these stress levels in the failure criterion gives the ultimate failure strength  $P$  of the loaded hole laminate. Figures 4-11 show the predicted strength ratios  $P/N_0$  for all the composite laminates listed in Table 1.

On inspection of the stress components at the weakest point of the notched laminate, keeping in view the ultimate failure strengths of the unnotched laminate in corresponding directions, the type of failure mode can be visualized. Figures 14 demonstrate this aspect for some of the laminates. In these figures, the values within the parentheses are ultimate failure strengths of unnotched laminates in MPa in corresponding directions. The dominant stress, contributing to the failure of the laminate has been underlined. Based on this observation, the modes of failure are also marked in Figures 4-11.

Experimental results for some of the laminates available in the literature are presented in the figures. For laminates  $(0,90 \pm 45)_S$  and

$(0, 90, (+45)_2)_S$ , the comparison is very good. Figure 4 depicts the strength ratio  $P/N_0$  versus diameter to width ratio  $D/W$  for  $(0, 90, +45)_S$  laminate. The experimental results taken from Reference 14, are based on the proportion transpired by the partial loading of the hole assuming 50% of the load transfer in two fastener hole laminates.

In the case of partial loading, as is shown in Figure 13 for AS-3501 material, the ultimate failure load of a loaded hole laminate is about 66% of the failure load of 0.5 hole load to total load ratio. This idea has been applied in calculating the failure strength of single fastener hole from two fastener hole experimental failure strength of the laminate. The other experimental result is taken from Reference 12 and is in the close proximity of predicted value. The predicted modes of failure are also the same as experimental observations. In Figure 5, the agreement between the predicted and experimental strengths and modes of failure is very good.

In Figures 6 and 8, the predicted strengths are conservative in comparison to experimental strengths. Probably it is due to the more nonlinear behavior of the composite laminates  $(0_2 \pm 45)_S$  and  $(90_2 \pm 45)_S$  when in compression. The predicted modes of failure resemble the experimental modes of failure. No experimental results are available for comparison with the predicted strengths of  $(0_2, 90_2)_S$ ,  $(+45)_2S$ ,  $(0^\circ)$ , and  $(90^\circ)$  - laminates for which the strength plots are given in Figures 7, 9, 10, and 11. It is expected that the predicted strengths are conservative, and thus are believed to be more reliable for design purposes.

Figure 12 shows the variation in ultimate failure strength  $P$  of loaded hole laminates with respect to the diameter to width ratio ( $D/W$ ). Predicted modes of failure are also marked for corresponding laminates in this figure.

Figure 13 gives the predicted and experimental (Reference 15) ultimate failure strengths of AS-3501,  $(0,90,\pm 45)_s$  - laminate with  $D/W = .125$  for partial loading of the hole. There exists a very good agreement between the predicted and experimental values.

Tables 3-4 give the comparison between predicted and experimental results for  $D/W = .125$ . The Table 3 results are for AS-3501 material  $(0,90,\pm 45)_s$  - laminate with four hole load to total load ratios. Experimental strengths for this case have been taken from Reference 15 and show a very good agreement with predicted strengths. Table 4 represents the experimental and predicted results for three different laminates of T300/5208 material. Experimental strengths are taken from Reference 12. The effect of some temperature and moisture contents is also included during strength calculations in these cases (Reference 16). It is seen that the results computed by using tensor polynomial failure criterion are conservative by a factor  $f_1$ , for dry room temperature; whereas this factor  $f_2$  is little less when some moisture and temperature change is introduced. However, since in composites, we find a great deal of scatter in ultimate strengths of laminates, it is not possible to get an exact agreement between the predicted and experimental results. Hence the comparison shown in this study is satisfactory.

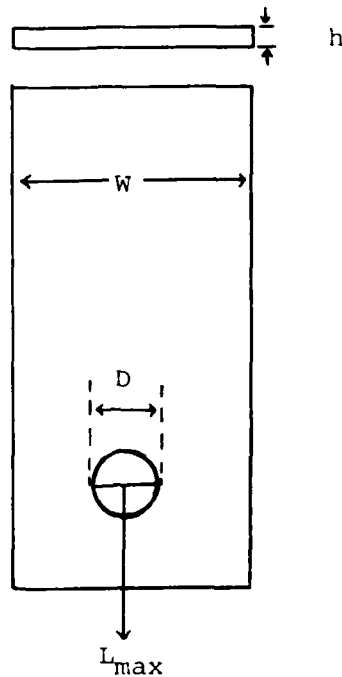
The forthcoming example demonstrates the use of design plots (Figures 4-11) in practical situations.

## 5. EXAMPLE

Given a  $(0,90,(\pm 45)_2)_s$  - laminate of T300/5208 material with a fastener hole. The hole diameter  $D$  is 5.08mm, width  $W$  of the laminate is 25.4mm and thickness  $h$  is 4.572mm. Using the design plot 5 and the strength of the unnotched laminate given in Table 2, compute the maximum allowable load that can be applied at the hole.

AFWAL-TR-80-4010

SOLUTION



$$D = 5.08\text{mm}$$

$$W = 25.4\text{mm}$$

$$h = 4.572\text{mm}$$

$$N_o = 505 \text{ MPa (from Table 2)}$$

$$= .102 \times 505 \text{ kgf mm}^{-2}$$

$$= 51.51 \text{ kgf mm}^{-2}$$

$$D/W = .2$$

$$\left(\frac{P}{N_o}\right)_{D/W=.2} = 1.05 \text{ (from Figure 5)}$$

$$P = 1.05 \times 51.51 \text{ kgf mm}^{-2} \text{ (maximum allowable stress)}$$

$$L_{max} = P \times h \times D$$

$$= 1256 \text{ kg}$$

Thus the maximum allowable load at the fastener hole is 1256 kg.

### SECTION III

#### CONCLUSIONS

The ultimate failure strengths and modes of failure of different composite laminates having a through the thickness loaded hole have been predicted using finite element method coupled with classical laminated plate theory and stress tensor polynomial failure criterion. The comparison between the predicted and experimental strengths is satisfactory. Design plots showing the ultimate strengths and modes of failure for various hole diameter to laminate width ratios are presented for a number of composite laminates made of T300/5208 material.

REFERENCES

1. B. Agarwal, "Static Strength Prediction of Bolted Joint in Composite Material," Presented at the AIAA Conference at St. Louis (1978) publication #79-0799.
2. S. P. Garbo and J. M. Ogonowski, Effects of Variances and Manufacturing Tolerances on the Design Strength and Life of Mechanically Fastened Composite Joints, AFFDL-TR-78-179, 1978.
3. J. M. Whitney and R. J. Nuismer, "Stress Fracture Criteria for Laminated Composites Containing Stress Concentrations," J. Composite Materials, Vol. 8 (1974), p. 253.
4. E. M. Wu, "Strength and Fracture of Composites," J. Composite Materials, Volume 5 (1974), p. 191.
5. R. Hill, The Mathematical Theory of Plasticity, Oxford University Press, London, 1950.
6. S. W. Tsai, "Strength Characteristics of Composite Materials," NASA Contractor Report, CR-224, April 1965.
7. S. W. Tsai and H. T. Hahn, "Recent Developments in Fracture of Filamentary Composites," paper presented at the International Conference on Prospects of Fracture Mechanics held at Delft University of Technology, The Netherlands, June 24-28, 1974.
8. S. W. Tsai and E. M. Wu, "A General Theory of Strength for Anisotropic Materials," J. Composite Materials, Vol. 5 (1971), P. 58.
9. S. W. Tsai, "Strength Ratios of Orthotropic Materials," Presented at Euromech Colloquium 115, Grenoble, France, June 1979.
10. E. M. Wu, "Fracture Mechanics of Anisotropic Plates," Composite Materials Workshop, edited by S. W. Tsai, J. C. Halpin, and N. J. Pagano, Technomic Publication, 1968.
11. S. W. Tsai and H. T. Hahn, Introduction to Composite Laminates, Air Force Materials Laboratory Technical Report, AFML-TR-78-201, Volume I, (1979).



REFERENCES (CONTINUED)

12. R. Y. Kim and J. M. Whitney, "Effect of Temperature and Moisture on Pin Bearing Strength of Composite Laminates," J. Composite Materials, Vol. 10 (1976), p. 149.
13. S. G. Lekhnitski, "Anisotropic Plates," translated from the Second Russian edition by S. W. Tsai and T. Cheron, Gordon and Beach, Science Publishers, New York, 1968.
14. E. R. Wogulis, "Advanced Composite Program for 737 Stabilizer," NASA-Boeing Critical Design Review, March 6-7, 1979.
15. Northrop Corporation Report, Advanced Composites Structural Mechanics, February/March 1979.
16. S. W. Tsai and H. T. Hahn, TI-59 Magnetic Card Calculator Solutions to Composite Materials, Air Force Materials Laboratory Report, AFML-TR-79-4040, April 1979.

PRECEDING PAGE BLANK - NOT FILLED

AFWAL-TR-80-4010

APPENDIX

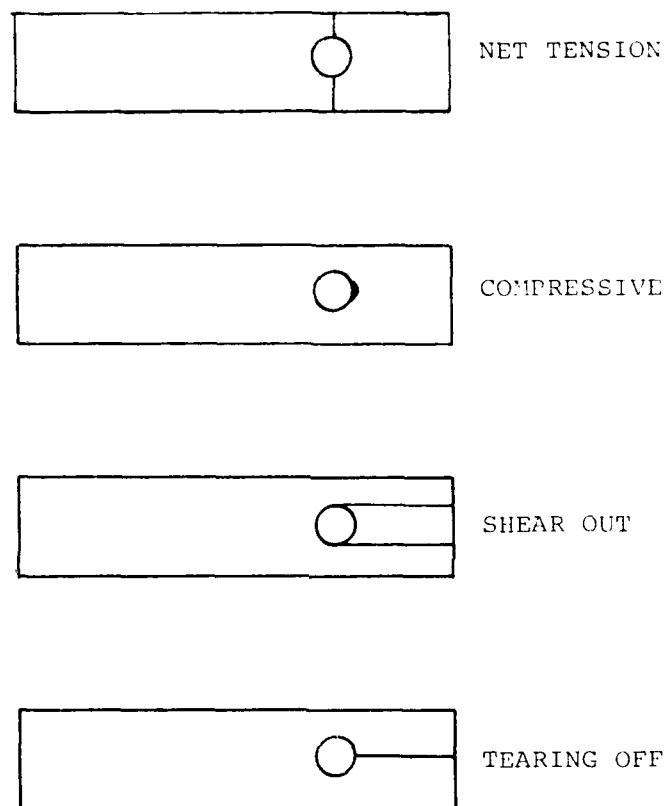


FIGURE A1. TYPES OF FAILURE MODE.

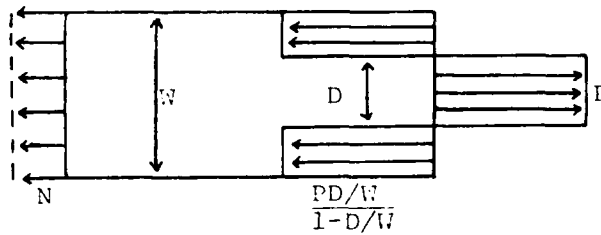


FIG. A2

NET TENSION:  $S_{cf} = \frac{D/W}{1-D/W}$

$P = N_O / S_{cf}$

(Refer Notations)

$\frac{P}{N_O} = \frac{1-D/W}{D/W}$

COMPRESSIVE:

$\frac{P}{N_O} = \frac{N_O^C}{N_O}$

SHEAR:  $\frac{P}{N_O} = \frac{N_O^S}{N_O}$

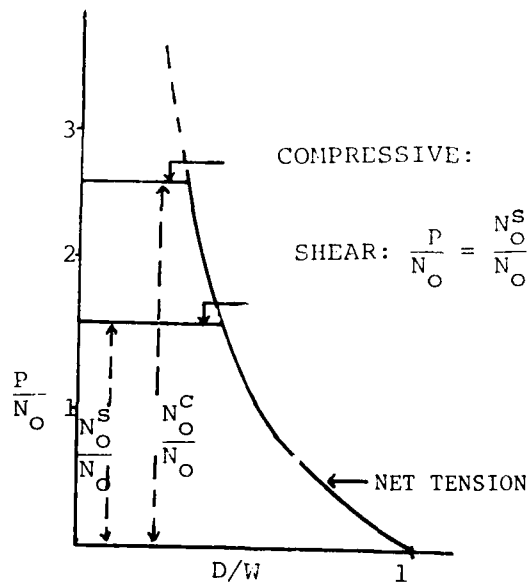


FIG. A3

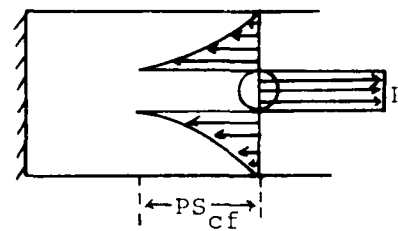


FIG. A4

NOTCH INSENSITIVE STRENGTH

TABLE 1  
MATERIAL PROPERTIES OF DIFFERENT  
LAMINATES IN SI-UNITS

Laminate	$Q_{11}^{\dagger}$ ( ————— GPa ————— )	$Q_{12}$	$Q_{22}$	$Q_{66}$	$N_o$ (MPa)
$(0,90,+45)_s$	76.368	22.607	76.368	26.88	582
$(0,90,(+45)_2)_s$	69.798	29.177	69.798	33.45	505
$(0_2,+45)_s$	119.234	22.607	33.502	26.88	960
$(90_2,+45)_s$	33.502	22.607	119.234	26.88	144
(0)	181.811	2.897	10.346	7.17	1500
(90)	10.346	2.897	181.811	7.17	40
$(+45)_{2s}$	56.658	42.318	56.658	46.59	123
$(0,90)_{2s}$	69.085	18.626	69.085	21.73	682

$$^{\dagger} \begin{bmatrix} \sigma_x \\ \sigma_y \\ \tau_{xy} \end{bmatrix} = \begin{bmatrix} Q_{11} & Q_{12} & 0 \\ Q_{12} & Q_{22} & 0 \\ 0 & 0 & Q_{66} \end{bmatrix} \begin{bmatrix} \epsilon_x \\ \epsilon_y \\ \gamma_{xy} \end{bmatrix}$$

TABLE 2  
FAILURE STRENGTHS OF DIFFERENT LAMINATES

<u>Laminate</u>	<u>No</u> <u>Tension</u> <u>(MPa)</u>		<u>No<sup>C</sup></u> <u>Compression</u> <u>(MPa)</u>	<u>No<sup>S</sup></u> <u>Shear</u> <u>(MPa)</u>
0°		1500	1500	68
90°		40	246	68
+45		123	149	856
(0 <sub>2</sub> , 90 <sub>2</sub> ) <sub>S</sub>	0	<u>682</u>	1108	68
	90	373	<u>2269</u>	68
(0 <sub>2</sub> , +45) <sub>S</sub>	0	<u>960</u>	536	255
	+45	515	<u>664</u>	<u>494</u>
(90 <sub>2</sub> , +45) <sub>S</sub>	90	115	<u>603</u>	255
	+45	<u>144</u>	322	<u>494</u>
(0, 90, +45) <sub>S</sub>	0	<u>582</u>	565	255
	90	276	<u>1298</u>	255
	+45	347	575	<u>494</u>
(0, 90, (+45) <sub>2</sub> ) <sub>S</sub>	0	<u>505</u>	400	317
	90	228	<u>946</u>	317
	+45	288	484	<u>615</u>

TABLE 3

COMPARISON BETWEEN EXPERIMENTAL AND PREDICTED  
STRENGTHS OF  $(0,90,+45)_s$  -AS-3501 LAMINATES  $D/W=.125$

<u>L<sub>ratio</sub></u> *	<u>P(ksi)</u> <u>Predicted</u>	<u>P(ksi)</u> <u>Experimental</u>	<u>f<sub>1</sub></u>
0	30.2 <sup>+</sup>	40 <sup>+</sup>	1.32
0.1	211.75	280	1.32
0.2	182.74	260	1.42
1	83.25	112	1.35

\*L<sub>ratio</sub> = Ratio of hole load to total load

+These values correspond to free hole case and thus act at the edge of the laminate.

TABLE 4

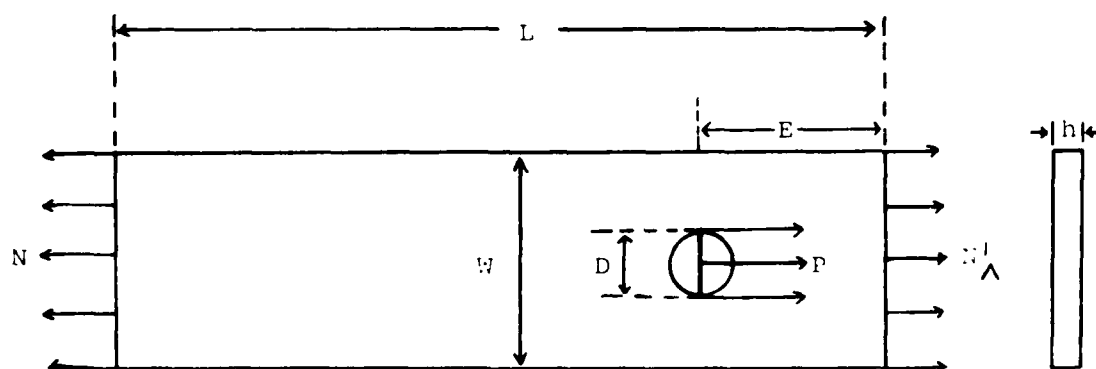
COMPARISON BETWEEN EXPERIMENTAL AND PREDICTED  
STRENGTH RATIOS FOR T300/5208 LAMINATE, D/W-.125

<u>Laminate</u>	<u>P/No</u> <u><math>\Delta T=C=0</math></u>	<u>P/No</u> <u><math>\Delta T=-150^{\circ}\text{C}</math></u> <u><math>C=.005</math></u>	<u>P/No</u> <u>Exp.</u>	<u><math>f_1</math></u>	<u><math>f_2</math></u>
$(0,90,+45)_s$	1.13	1.12	1.35	1.19	1.21
$(0_2,+45)_s$	.33	.35	.72	2.18	2.06
$(90_2,+45)_s$	1.51	1.67	2.63	1.74	1.57

$$f_1 = (P/No)_{\text{Exp.}} / (P/No)_{\Delta T=C=0}$$

$$f_2 = (P/No)_{\text{Exp.}} / (P/No)_{\Delta T=-150^{\circ}\text{C}, C=.005}$$





$L = 13.3 \text{ cm}$   
 $h = 0.2032 \text{ cm}$   
 $W = 2.54 \text{ cm}$   
 $E = 0.894 \text{ cm}$   
 $D = 0.3175 \text{ to } 0.9 \text{ cm}$

Figure 1. Laminate with Coordinate Axis and Dimensions

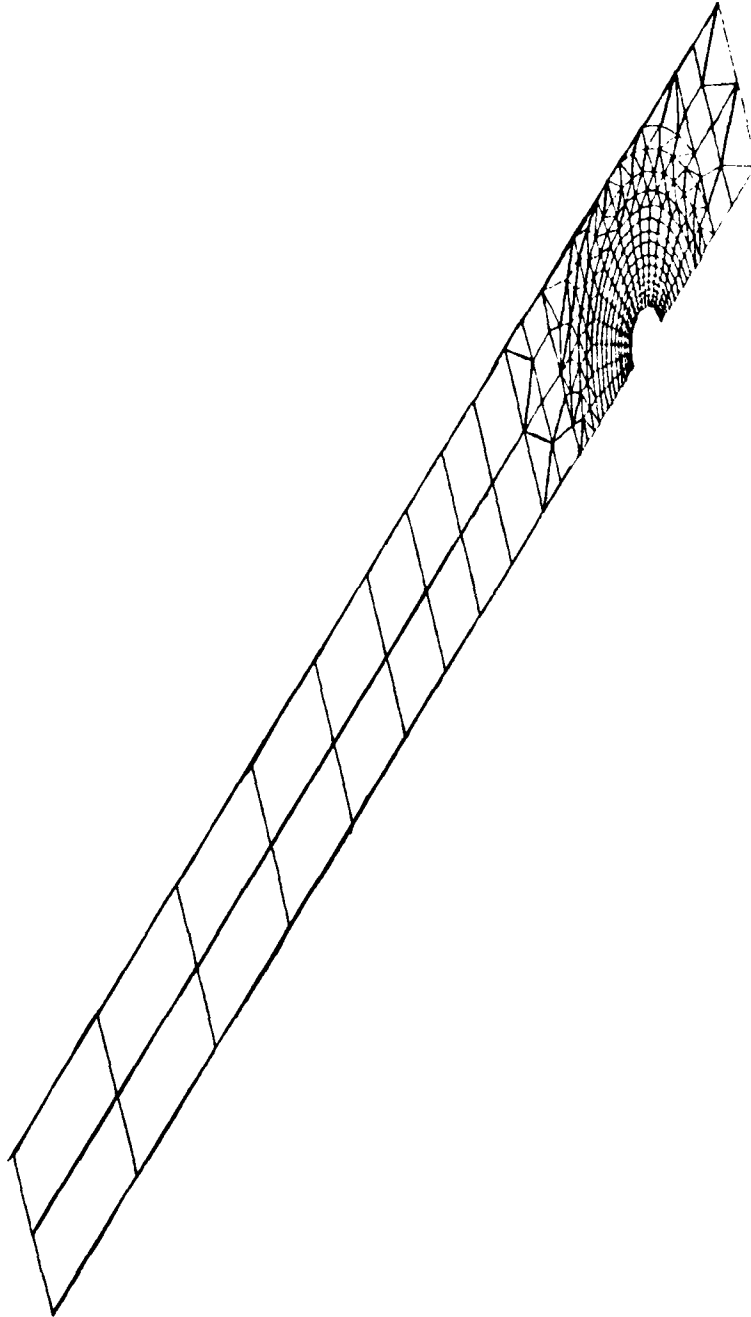


Figure 2. Finite Element Grid of the Laminate

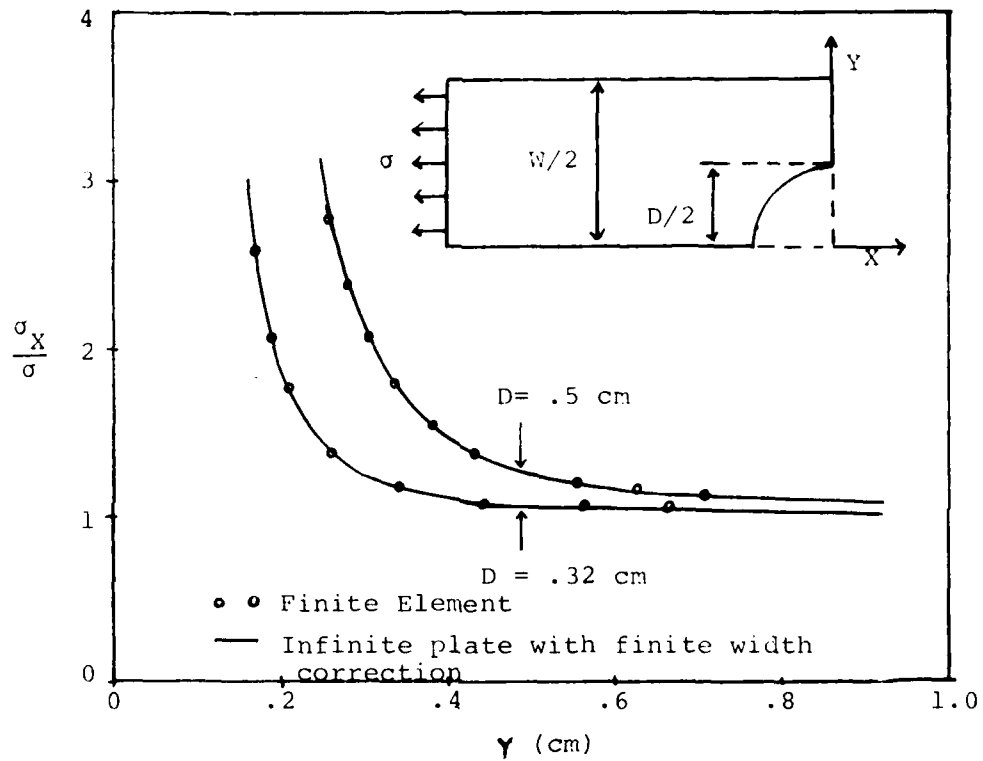


Figure 3. Comparison Between Finite Element and Closed Form (with a Finite Width Correction Factor) Results for  $\sigma_x$  in Free Hole Boundary Condition

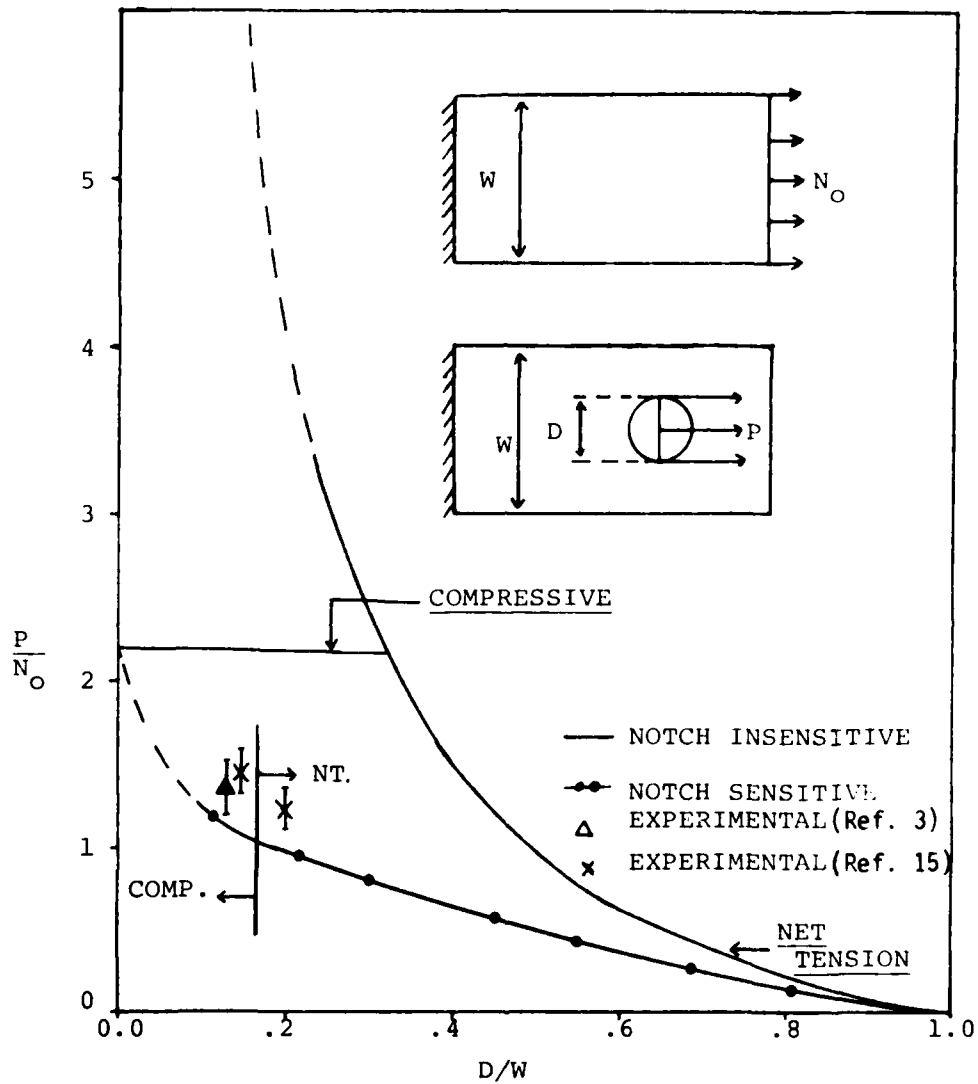


Figure 4. Strength Ratio  $P/N_0$  versus Diameter to Width Ratio  $D/W$  of the  $(0,90,+45)_s$  Laminate

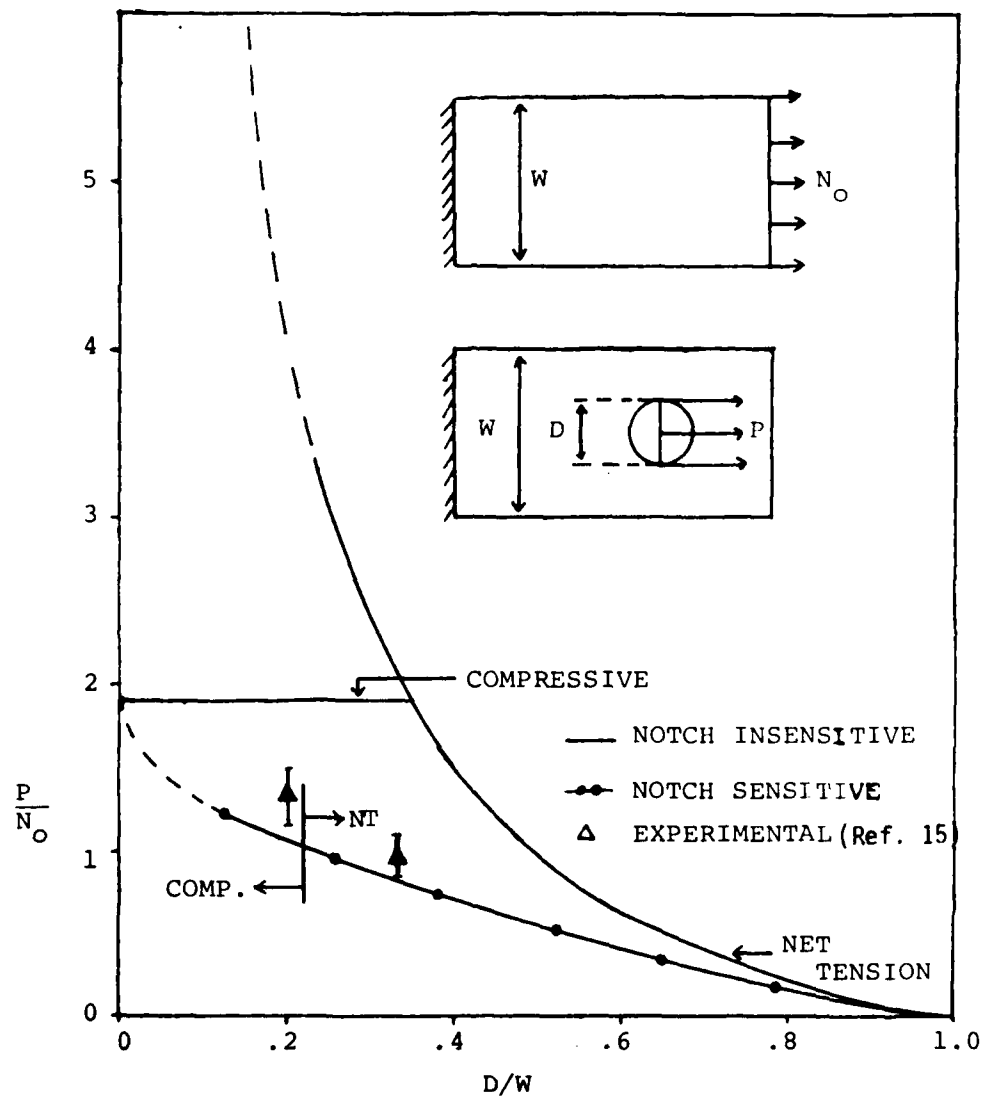


Figure 5. Strength Ratio  $P/N_0$  versus Diameter to Width Ratio  $D/W$  of the  $(0,90,(+45)_2)_S$  Laminate

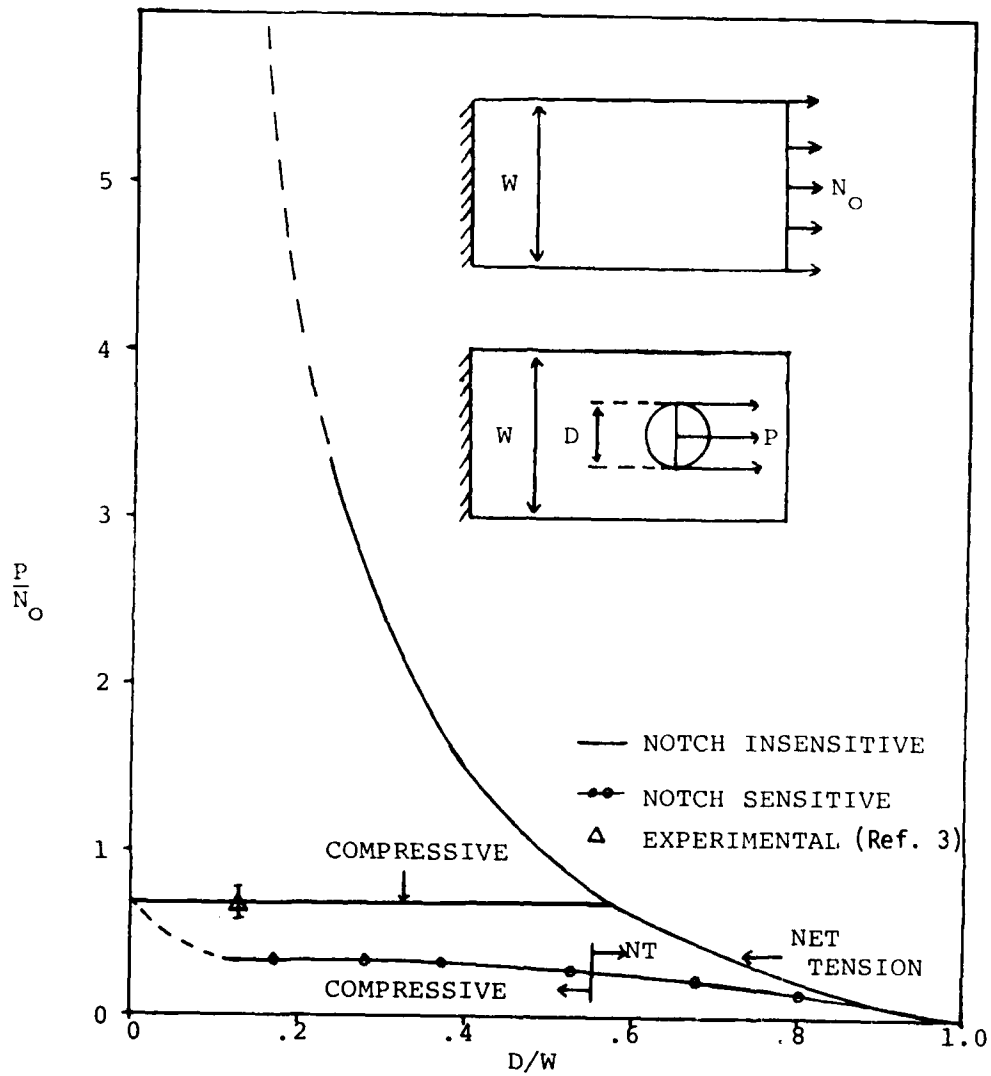


Figure 6. Strength Ratio  $P/N_0$  versus Diameter to Width Ratio  $D/W$  of the  $(0_2, +45)_s$  - Laminate

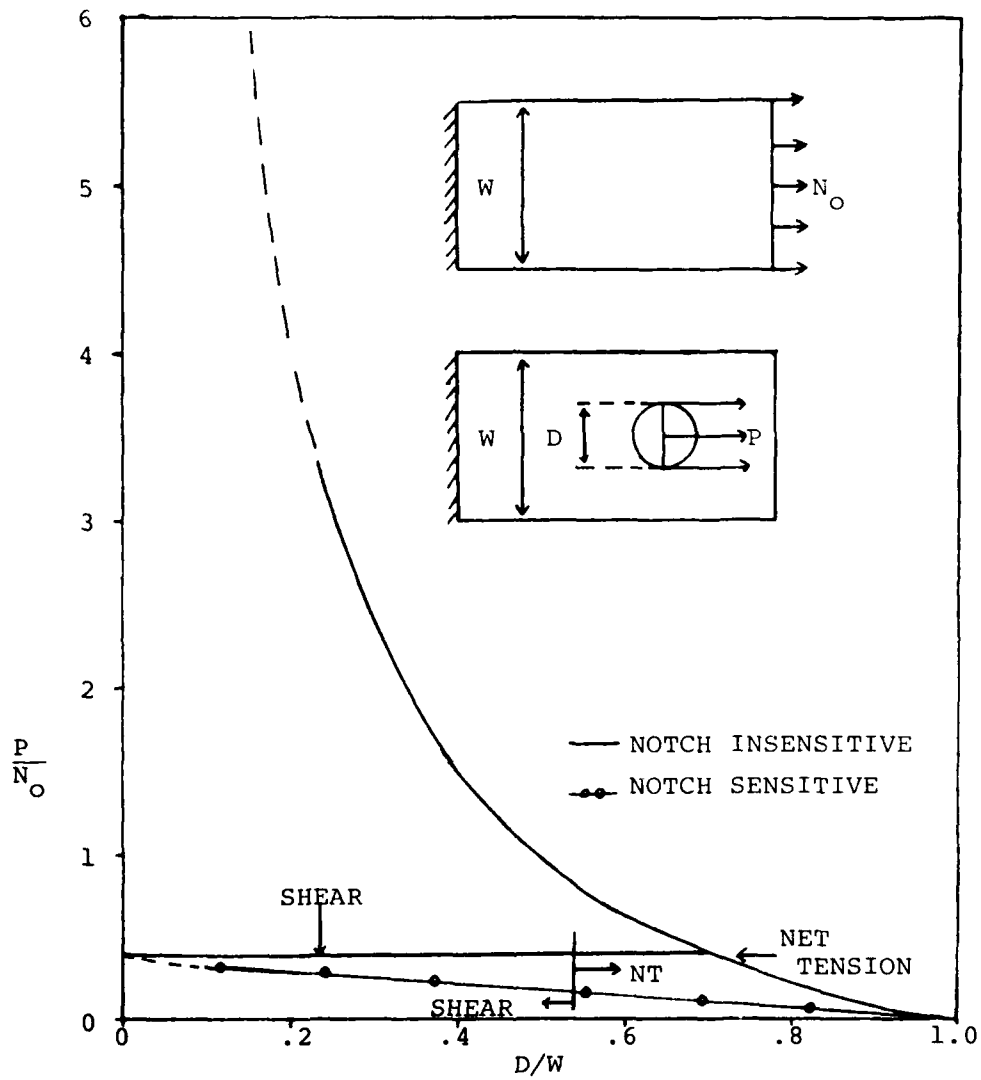


Figure 7. Strength Ratio  $P/N_0$  versus Diameter to Width Ratio  $D/W$  of the  $(0,90)_{2s}$  Laminate

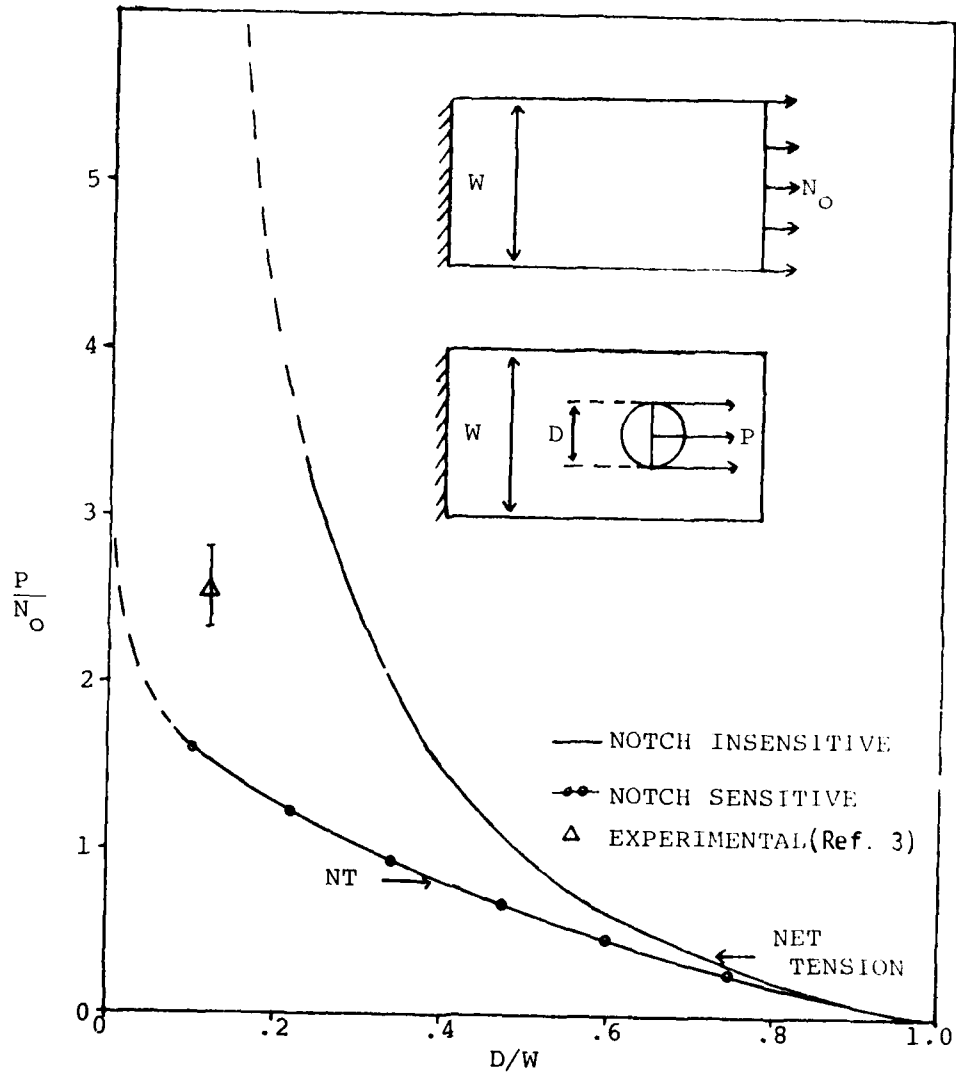


Figure 8. Strength Ratio  $P/N_0$  versus Diameter to Width Ratio  $D/W$  of the  $(90_2, \pm 45)_s$  Laminate



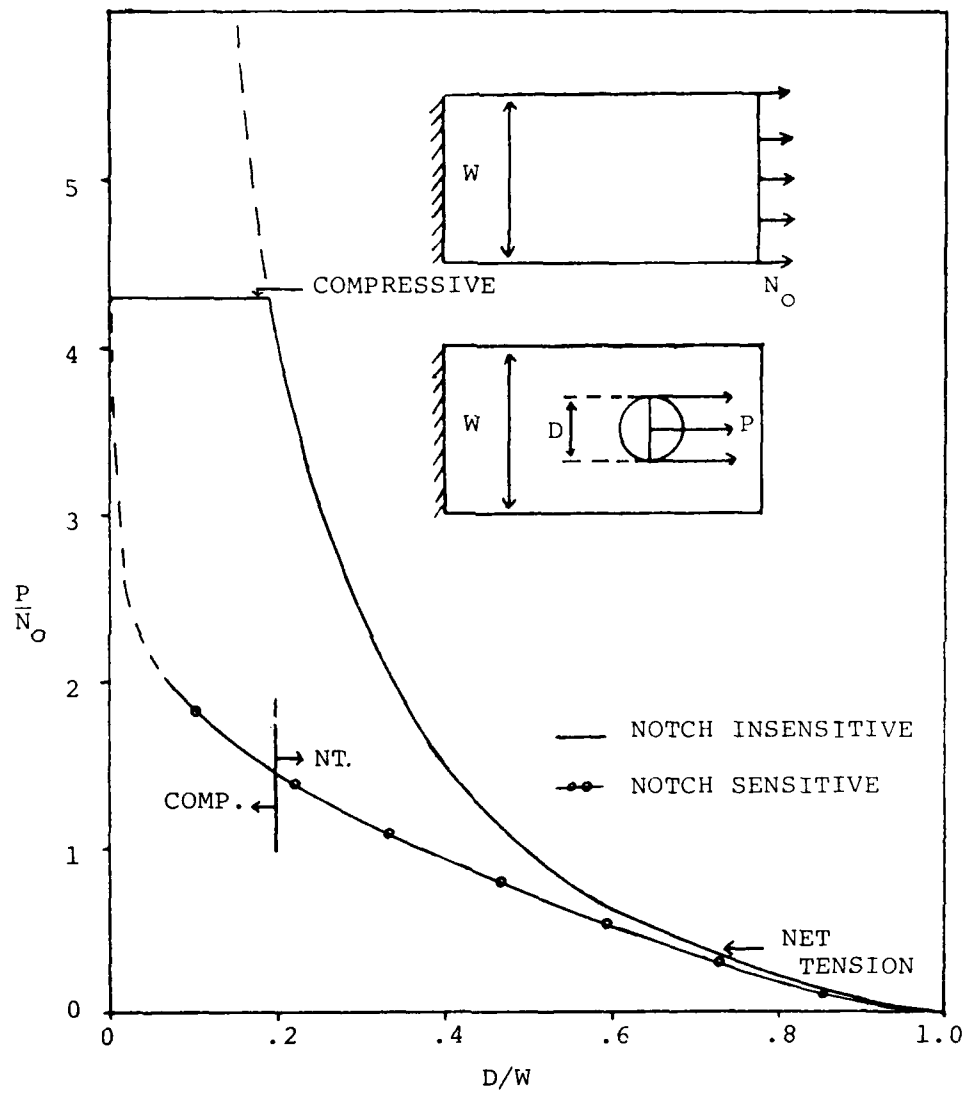


Figure 9. Strength Ratio  $P/N_0$  versus Diameter to Width Ratio  $D/W$  of the  $(+45)_{2s}$  Laminate

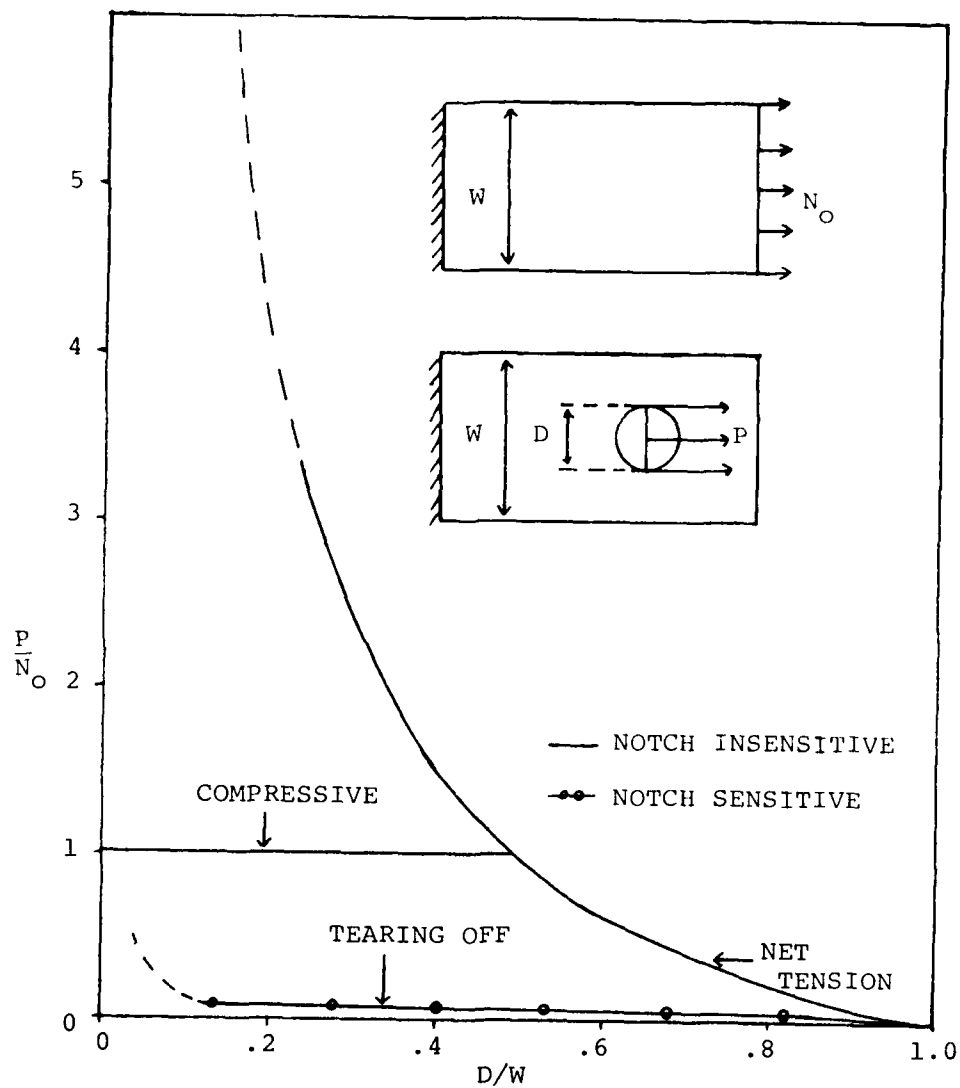


Figure 10. Strength Ratio  $P/N_0$  versus Diameter to Width Ratio  $D/W$  of the  $(0^\circ)$  Laminate

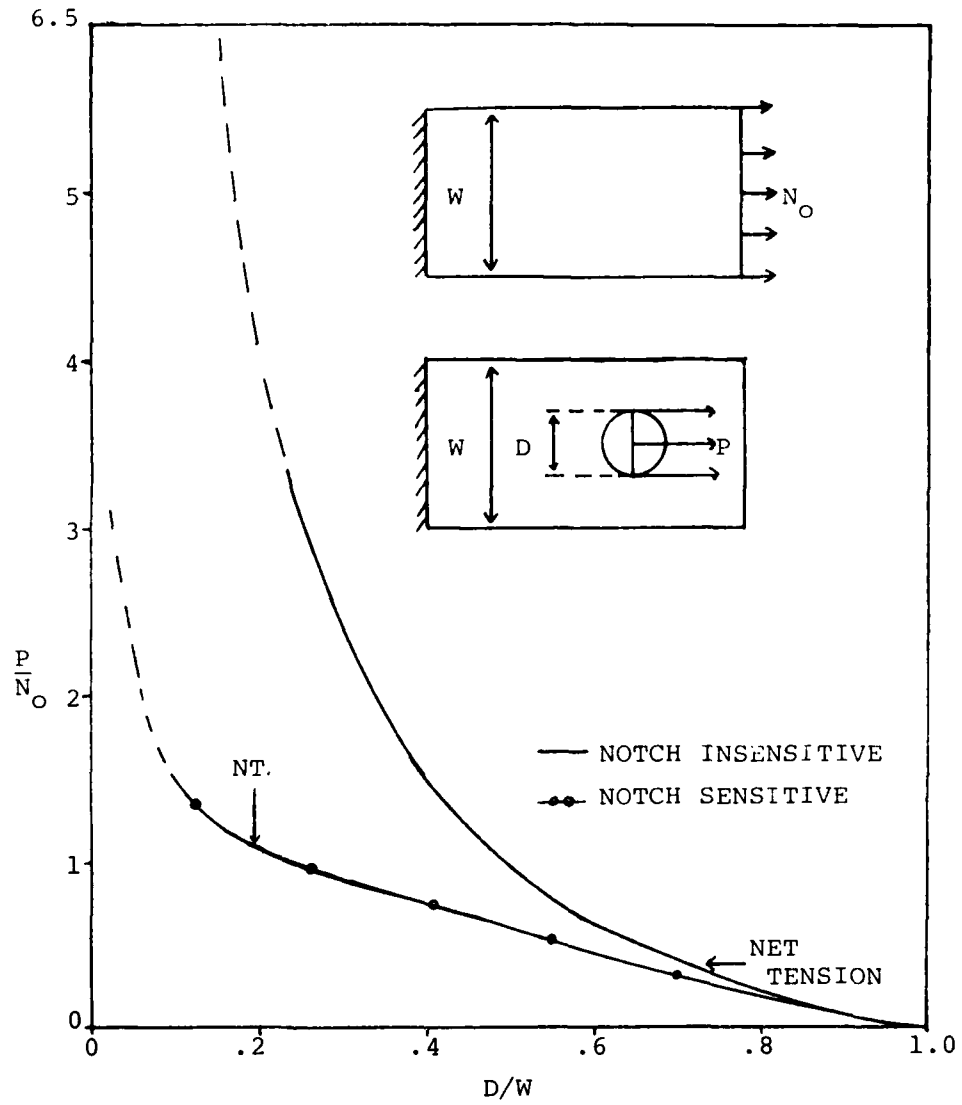
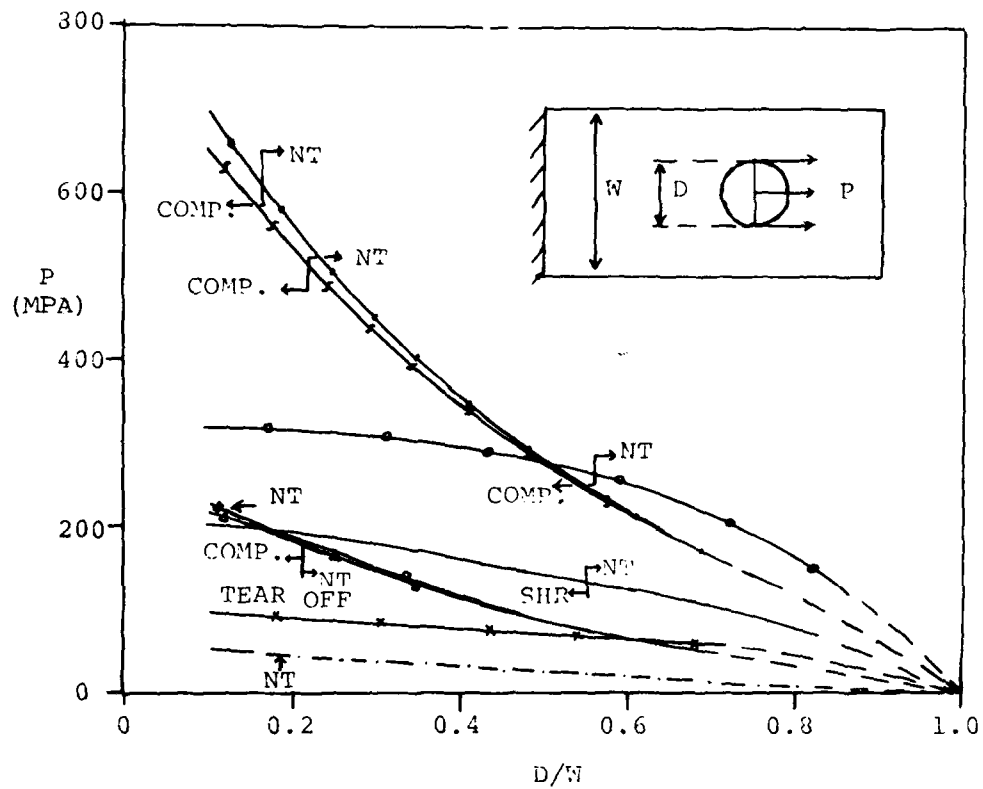


Figure 11. Strength Ratio  $\frac{P}{N_0}$  versus Diameter to Width Ratio  $\frac{D}{W}$  of the  $(90^\circ)$  Laminate



$(0,90,+45)_S$ ;  $++$ ,  $(0,90,(+45)_2)_S$ ;  $oo$ ,  
 $(0_2,+45)_S$ ;  $-$ ,  $(0,90)_2S$ ;  $o-o$ ,  $(90_2,+45)_S$ ;  
 $\Delta\Delta$ ,  $(+45)$ ;  $***$ ,  $(0)$ ;  $---$ ,  $(90^\circ)$ .

Figure 12. Strength  $P$  versus Diameter to Width Ratio  $D/W$  of Various Angle Ply Laminates

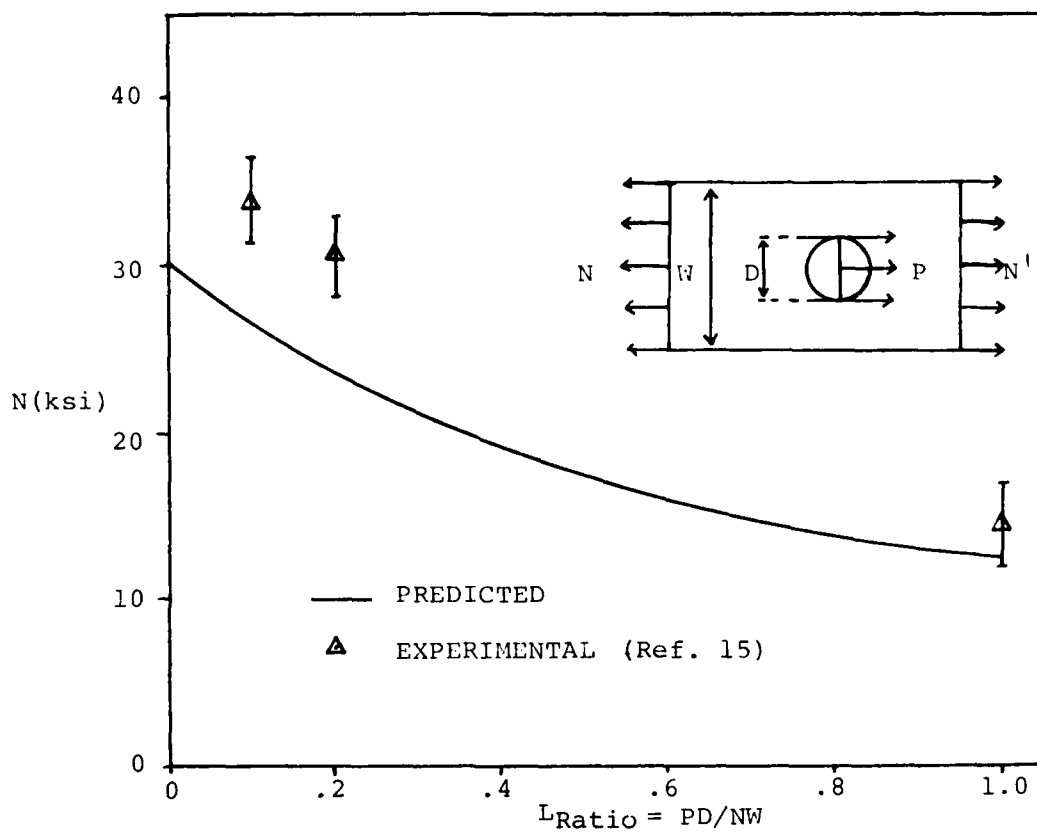


Figure 13. Strength  $N$  versus Hole Load to Total Load Ratio of AS-3501 Material (0,90,+45)<sub>s</sub> Laminate,  $D/W = .125$

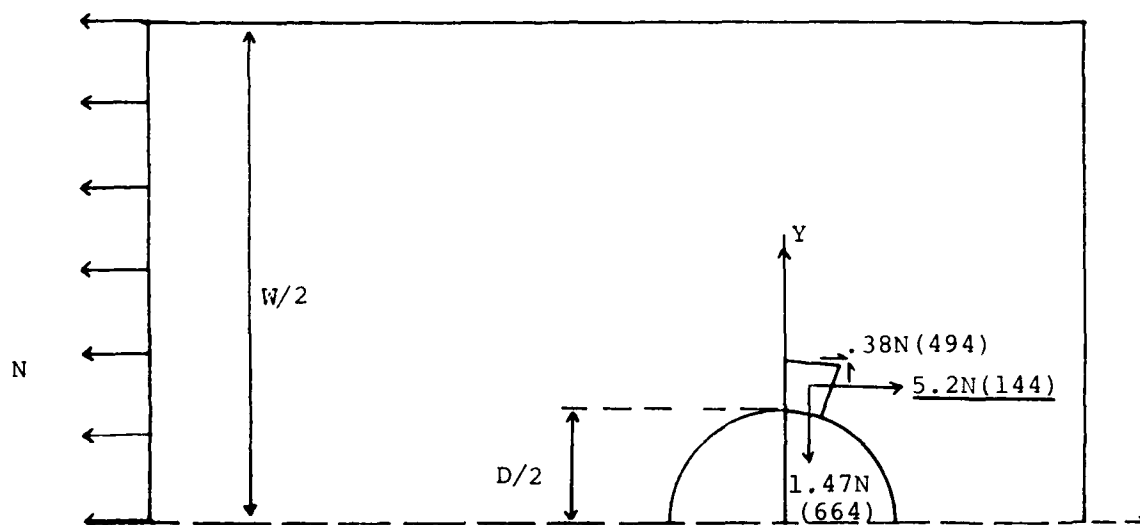


Figure 14 (a). Projection of Failure Mode for  $(90_2, +45)_s$  Laminate,  $D/W = .125$ . Net Tension Failure.

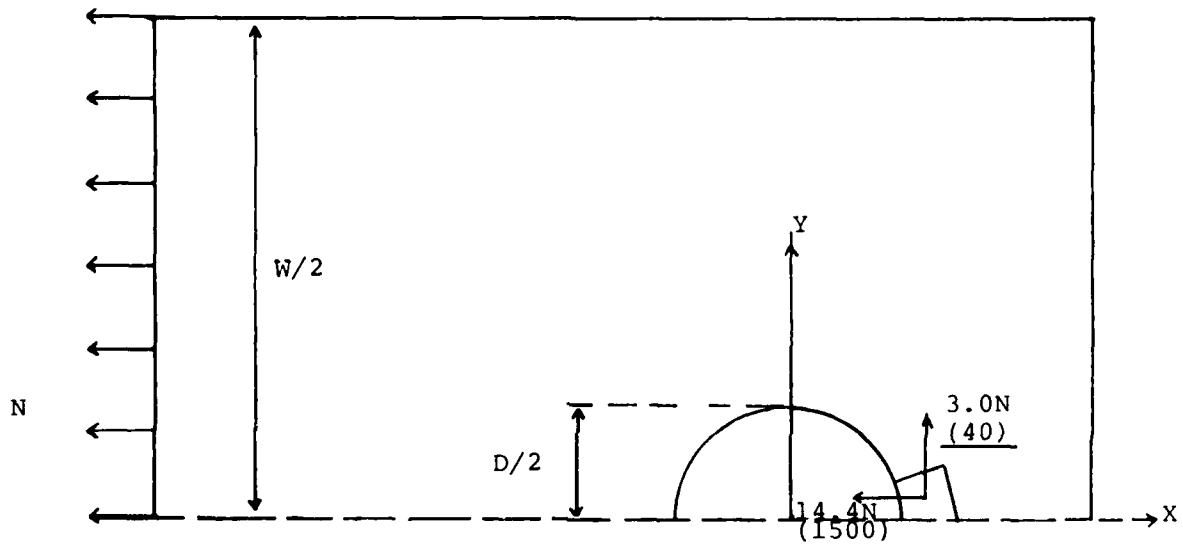


Figure 14 (b). Projection of Failure Mode for (0)-Laminate,  $D/W=.125$ . Tearing Off Failure.

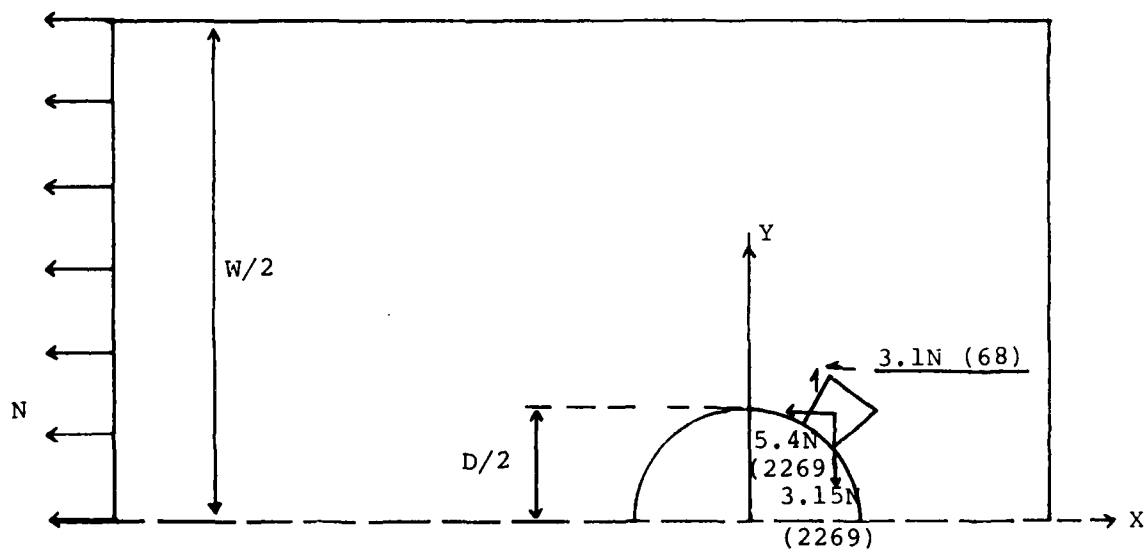


Figure 14 (c). Projection of Failure Load for  $(0,90)_{2s}$  Laminate,  $D/W = .125$ . Shear Out Failure.



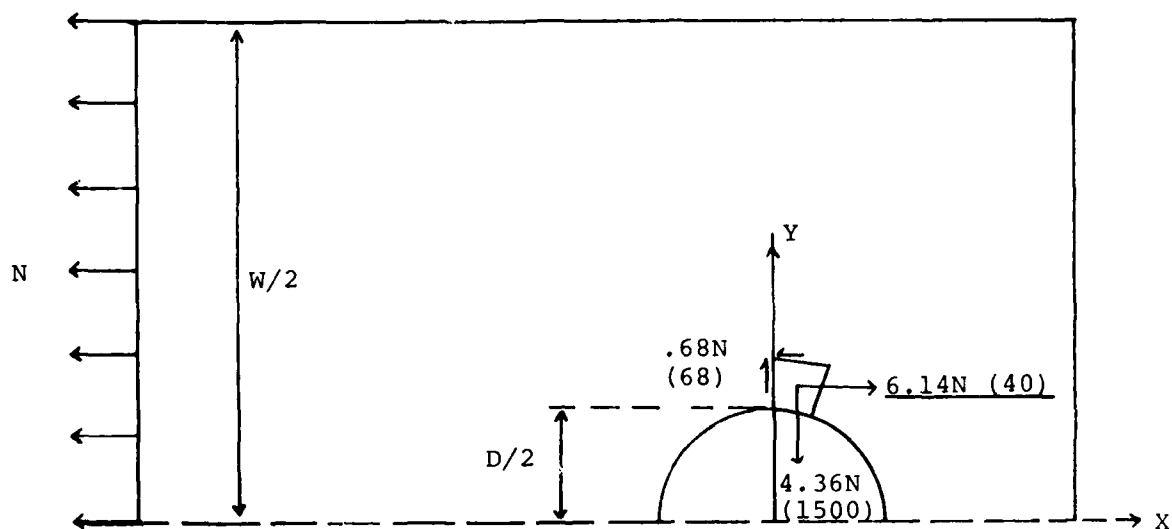


Figure 14 (d). Projection of Failure Mode for  $(90^\circ)$  Laminate,  $D/W = .125$ . Net Tension Failure.

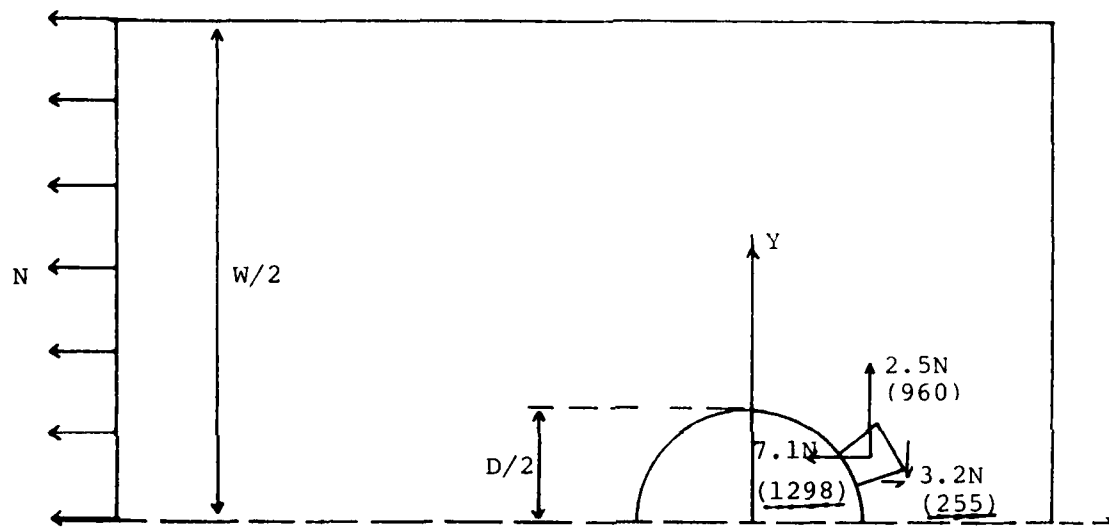


Figure 14 (e). Projection of Failure Mode for  $(0,90,+45)_s$  Laminate,  $D/W = .125$ . Compressive Failure.

ATE  
LMED  
-8